An Ultra-Thin Low-Frequency Tunable Metamaterial Absorber Based on Lumped Element

GuoWen ZHANG, Jun GAO, Xiangyu CAO, HuanHuan YANG, Liaori JIDI

Information and Navigation College, Air Force Engineering University, Fenghao Road 1st Xi'an 710077, China

849325138@qq.com, gjgj9694@sina.com, xiangyucaokdy@163.com, jianye8901@126.com, jidiliaorikdy@163.cm

Submitted January 17, 2019 / Accepted June 19, 2019

Abstract. *In this paper, an ultra-thin metamaterial absorber with a stretching transformation (ST) pattern is proposed and fabricated in the low-frequency range. The absorber is composed of dielectric layer, metal patch loading resistor and variable capacitor which produce its tunability. In order to expand the tunable bandwidth, we applied the ST with various coefficients x and y to the unit cell pattern. Measurement and simulated results show that the structure can be tuned to provide a continuously variable reflectivity level of less than –10 dB from 0.68 to 2.13 GHz at bias voltages of 10–40 V. The total thickness of this absorber was only λ/31 of the center frequency. Both measurements and simulated results indicate that this absorber can be thin and achieve a tunable absorption simultaneously.*

Keywords

Low-frequency, wideband, ultra-thin, ST coefficients, tunability

1. Introduction

Metamaterial absorbers (MAs) can efficiently dissipate the electromagnetic (EM) energy into heat, resulting in significant reduction of the reflected waves along the echo direction. However, limited to thickness and narrow bandwidth at frequencies below 3 GHz, the MAs will be difficult to be used in practice applications. Thus, MAs with small size and broadband absorption are urgently necessary.

The perfect metamaterial absorber [1] concept was first reported by Landy et al. In the microwave regime, this seminal work soon inspired work in other frequency ranges from terahertz to visible regime due to their potential application [2]. Among these MAs, since microwave MAs are thinner and lighter than the traditional microwave absorbers and can be used in military and commercial areas, which have been become a new research hot topic [3–7]. So far, several methods in common have been devoted to accomplish the wideband absorber. For instance, the absorption bandwidth can be broadened by constructing the metamaterial absorber array with periodic arrangement or superimposing the different resonance modes within a unit cell [8], [9]. Additionally, the fractal metal structures [10] and the multilayer [11–13] were realized to design wideband absorber. As a remarkable method, loading with lumped element was utilized to achieve broadband absorption [14–16]. Although many efforts towards the improvement of the performance about MAs are flourishing, the low-frequency and broadband absorber are not easily realized without lumped elements or increasing material thickness.

In this work, we present an ultra-thin MA with a stretching transformation (ST) pattern for use in low-frequency applications. The total thickness 6.036 mm is only λ/31 of the center frequency. Using the transmission line (TL) model, we can get the relationship between the resonant frequency and the real part of the input impedance. The equivalent circuit model is introduced to analyze the broadband and tunable absorption for the proposed MA. Then, we change the ST coefficients of unit cell pattern to expand the tunable bandwidth. Finally, we also fabricated and measured the proposed ultra-thin MA. The experiment results are given to validate the good performance of the MA.

2. Design and Analysis

A schematic of the proposed MA is depicted in Fig. 1(a), which is composed of the dielectric substrate sandwiched with periodic metal electric resonator loaded with resistors and capacitors and ground plane. The material of dielectric substrate is F4BM with dielectric constant 2.65 and the loss tangent is 0.001. Metal patch loaded with resistors and capacitors was placed above the dielectric layer. The middle layer is air and the bottom layer is a full metallic plate. The metallic structures and ground are coppered with conductivity of 5.8×10^7 S/m and the thickness of 0.036 mm. The MA is simulated and optimized. A full-wave electromagnetic simulation is performed by using finite-element analysis based High Frequency Structure Simulator (HFSS 14.0). The periodic boundary conditions (PBCs) and Floquet port are utilized to simulate the infinite periodic cells. The resistor and capacitors are simulated using a lumped LRC model. The optimized parameters of

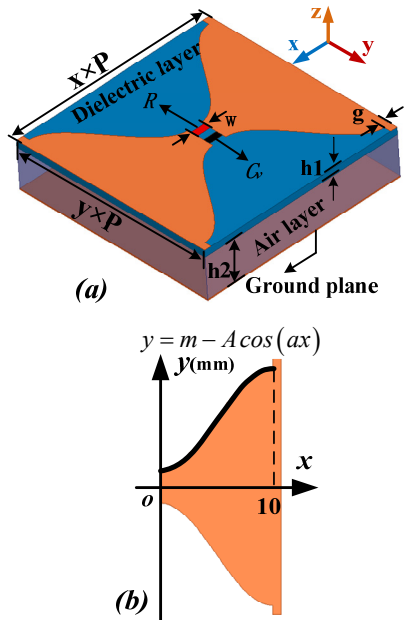

Fig. 1. Schematic geometry of the MA. (a) The geometry of the unit cell. (b) The curve of metallic plate.

metallic structures are as follows: $p = 30$, $h1 = 1$, $h2 = 5$, $w = 2$, $g = 1$, $m = 14$, $A = 12$, (units: mm) and $x = 0.8$, $y = 1$, $a = \pi/10$. Figure 1(b) shows the boundary curve function of metallic plate.

In the simulation process, the master-slave boundary is applied to replicate an infinite planar array, and the incident wave is a plane wave with a linear polarization along the $(-z)$ direction. Then, the absorbance of MA $A(\omega) = 1 - T(\omega) - R(\omega)$ is calculated using the frequency-dependent transmittance $T(\omega) = |S_{21}(\omega)|^2$ and reflectance $R(\omega) = |S_{11}(\omega)|^2$ obtained from the simulation. The transmission is zero $(T(\omega) = |S_{21}(\omega)|^2 = 0)$ attributed to the metallic plate without patterns on the bottom layer. Thus, the absorbance can be calculated using $A(\omega) = 1 - R(\omega)$. In effective medium theory, effective permittivity $(\varepsilon = \varepsilon' + j\varepsilon'')$ and effective permeability $(\mu = \mu' + j\mu'')$ are generally used to analyze absorptivity, because the characteristic impedance of a material can be defined as $Z(\omega) = [\mu(\omega)/\varepsilon(\omega)]^{1/2}$. But in some cases, electromagnetic parameters are not readily available. So the TL model is a powerful tool to interpret this structure.

From Fig. 2(b), we realized that the resonance state exists and may be important for deep absorption. With $R = 600\ \Omega$, the absorbability was relatively good. Figure 2(a) shows the resonance frequency varies with capacitance when $R = 600\ \Omega$. To numerically analyze the absorption performance, we establish an accurate model for MA. Figure 3(a) shows the equivalent circuit model of MA based on TL theory [17]. By derivation, the equivalent impedance of MA can be expressed by the following formula:

$$Z_{MA} = \frac{R}{(C_d + C_V)^2 R^2\omega^2 + 1} + \frac{1}{j\omega}\left[\frac{C_d + C_V}{(C_d + C_V)^2 + 1/R^2\omega^2} - L_d\omega^2\right]. \quad (1)$$

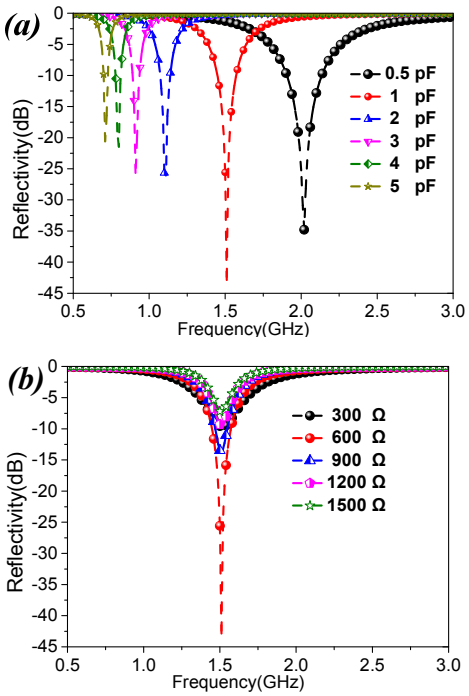

Fig. 2. Simulated reflectivity of the MA with the value of one parameter changed while the values of others unchanged: (a) R, (b) C_v.

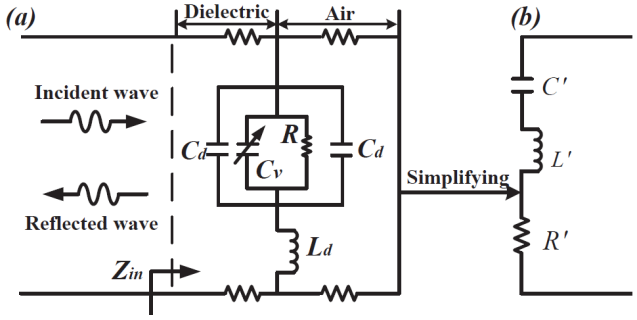

Fig. 3. Equivalent circuit of MA. (a) Equivalent circuit model. (b) Simplified equivalent circuit model.

The distributed parameters L_d and C_d are constant which is determined by the structure with $x = y = 1$. The values of lumped elements are R and C_v, respectively. The real part of Z_{MA} can be substituted with a resistor R', and the imaginary part of Z_{MA} is a capacitor C'. ω is the angular frequency of the electromagnetic wave. R' and C' are described by:

$$R' = \frac{R}{(C_d + C_V)^2 R^2\omega^2 + 1}, \quad (2)$$

$$C' = 1\Big/\left[\frac{C_d + C_V}{(C_d + C_V)^2 + 1/R^2\omega^2} - L_d\omega^2\right]. \quad (3)$$

Figure 3(b) shows the simplified equivalent circuit model. The resonance frequency f of the simplified circuit is described as:

$$f = \frac{\sqrt{1\Big/\left(C'L' - C'^2R'^2\right)}}{2\pi}. \quad (4)$$

According to (2), (3), (4), the real of equivalent impedance at resonance frequency can be expressed by the following formula:

$$\mathrm{Re}\left(Z_{\mathrm{MA}}\right)=1+\frac{1}{4\pi^2 f^2 C'^2 R'}. \tag{5}$$

ST is applied to the unit cell pattern. The size of the unit cell is $(x \times P)$,$(y \times P)$, where P is the basic size before ST and x and y are the ST coefficients on each side. The topological structure of the MA pattern significantly affects the resonant frequency of the absorber. A larger unit cell will have a lower resonance frequency. L_d and C_d represent the distributed parameters, including inductance and capacitance. When the input impedance of the MA matches with that of free space, the real part will be 377 Ω and the imaginary part will be 0. According to (2), (3), (5), the resonance frequency f and the real part at resonance $\mathrm{Re}(Z_{\mathrm{MA}})$ are functions of L_d, C_d, C_v, and R. In this case, the resonance frequency f and $\mathrm{Re}(Z_{\mathrm{MA}})$ depend only on the lumped elements C_v and R.

The resonance frequency f varies with the capacitance of the varactor C_v as shown in Fig. 4.When the value of resistance was fixed at 600 Ω, the simulated curve with various C_v was shown in Fig. 4(a), which coincided well with the calculated curve. The calculated curve of f–C_v in Fig. 4(b) was calculated according to (4), which described that the resonant point is a descending function of C_v.

Figure 5 shows the relationship between f and R. With C_v = 1 pF, we get R-f curves when R changes from 300 to 1500 Ω, as shown in Fig. 5(a). Figure 5(b) shows the simulated results for various R by the TL model. The resulting curve both simulated and calculated described that varying R affects f only slightly. So we can approximate f as just a function of C_v.

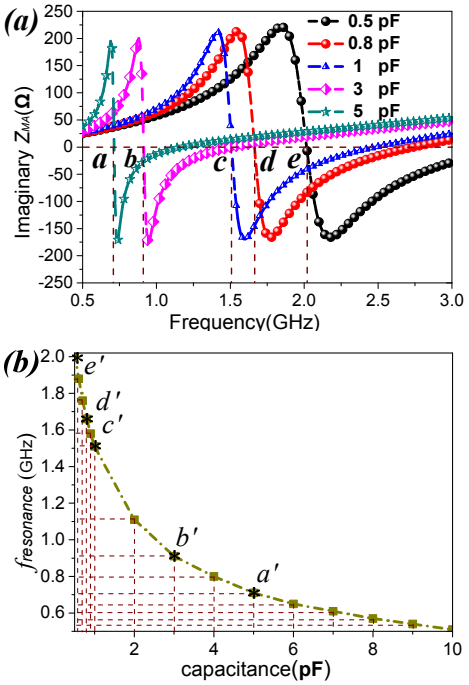

Fig. 4. The curves of f and C_v: (a) Calculated by the HFSS. (b) Simulated results calculated by using the TL model.

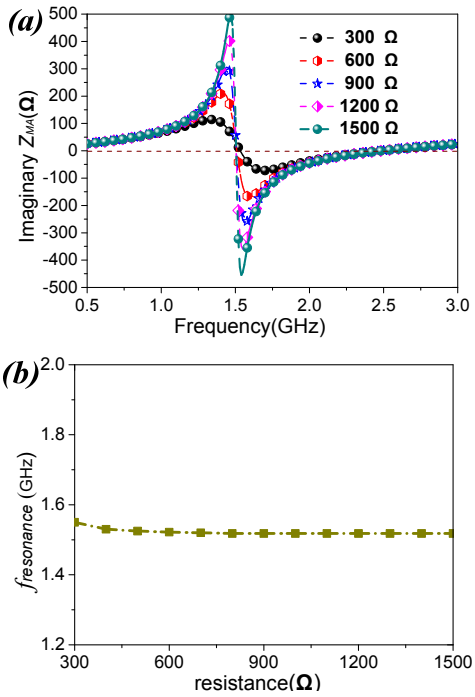

Fig. 5. The curves of f and R: (a) Calculated by the HFSS. (b) Simulated results calculated by using the TL model.

The relationship between the impedance $\mathrm{Real}(Z_{\mathrm{MA}})$ and R, C_v are depicted in Fig. 6. It can be seen from Fig. 6(a) that the real part of impedance at resonant frequency is almost constant with the varying of C_v. Figure 6(b) shows the relationship between $\mathrm{Real}(Z_{MA})$ and R when the MA resonates. From this we can see that the real part of the impedance varies sharply with the value of resistance.

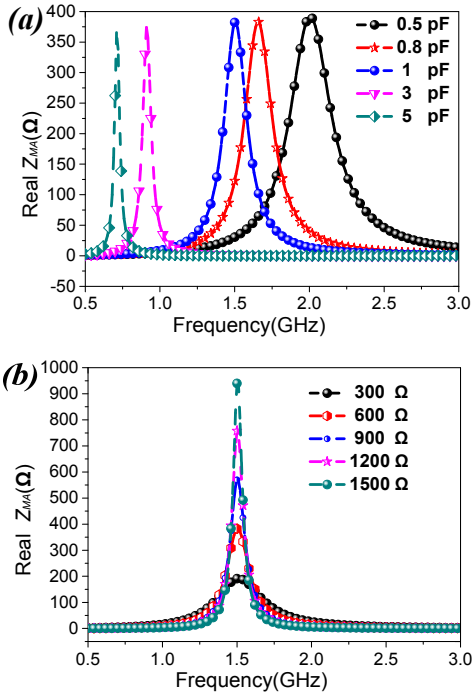

Fig. 6. The curves of Real (Z_{MA}) and R, C_v. (a) Real (Z_{MA})-C. (b) Real (Z_{MA})-R.

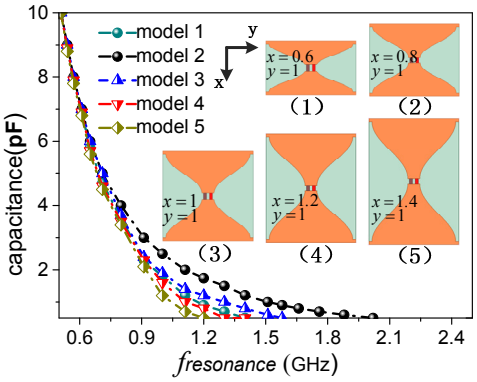

Fig. 7. The curves of $f_{resonance}$–C_v with different patterns.

On the whole, the resonance frequency f is mainly contacted to C_v, while the real part of Z_{MA} at resonance frequency is mainly related on R. The MA which is loaded with a resistor and varactor is designed with a tunable absorber. Using the varactor which provided a variable capacitance at varying bias voltages produces the device's tunability. Resistor reliably generated strong absorption at the resonance frequency, which is realized by using a lumped constant resistance.

It makes sense to expend the tunable bandwidth of MA, based on our qualitative analysis of R and C_v. In addition to resistor and capacitor, the structure parameters also have a greater impact on the absorption characteristics. Through varying ST coefficients of the unit cell pattern, the tunable bandwidth can be expanded. We designed five patterns in Fig. 7. The curve of resonance frequency changing with capacitance value under different patterns was shown in Fig. 7. These patterns are conversions of the pattern shown in Fig. 1(a). As we can see from the figure, when the capacitance varies from 0.5 pF to 5 pF, the model 2 has the widest tunable bandwidth.

3. Simulation and Discussion

The feasibility of the proposed absorber is demonstrated by prototypes with the size of 300 mm × 288 mm. The prototypes of absorber have been fabricated using a common printed circuit board method on the substrates with the thicknesses of 1 mm and they are illustrated intuitively in Fig. 8(a), where the ST coefficients are $x = 0.8$, $y = 1$. Capacitance is controlled by using bias line to load different voltages. The bias lines with the same voltage are connected together. The measurement setup is composed of a vector network analyzer (Agilent N5230C) and two linear polarized standard-gain horn antennas. The antennas are placed vertically to the sample to ensure normal incidence. One horn antenna is used to transmit, and the other horn antenna receives the reflected waves. Figure 9 shows the measured reflectivity curves of MA for different voltage. As we changed voltage from 10 to 40 V using the power control system, the resonant point covered a frequency band of 0.68–2.13 GHz with the reflectivity below –10 dB. The experimental results show good agreement with the simulated results. There are small discrepancies such as the

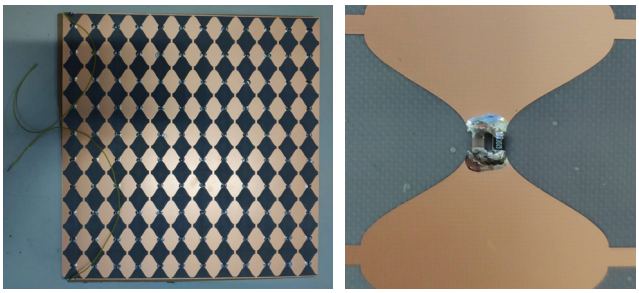

Fig. 8. (a) Photograph of the MMA sample. (b) Magnified picture of the unit cell.

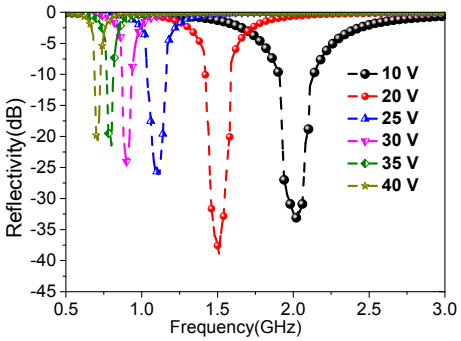

Fig. 9. The measured reflectivity of the tunable MA.

depth of the peak but these discrepancies can be accepted in both the simulation and the measurement system.

For comprehensive comparison, we define the relative volume Rv of a unit cell as follows:

$$Rv = Tv/(\lambda_0)^3 \tag{6}$$

where λ_0 is the wavelength of the center frequency for absorption bandwidth and Tv is the total volume of a unit cell. In order to synthesize the relative absorption bandwidth BW of these absorbers in reference, we have evaluated the cost-efficient bandwidth BW_{CE} defined as:

$$BW_{CE} = BW / Tv\,. \tag{7}$$

In reference, the resistive surface has been applied for increasing absorption bandwidth. Obviously, the intrinsic advantages of the proposed absorber include not only that it can be easily implemented using the inexpensive printed circuit board fabrication techniques but also that it exhibits low-profile and wideband absorption. From Tab. 1, it is seen that our proposed design performs the smallest relative volume Rv and the most cost-efficient bandwidth BW_{CE} (3295.5) of a unit cell.

ID	Frequency range (GHz)	Total thickness (mm)	Relative volume of a unit cell	Cost-efficient bandwidth
[4]	1.85~4.45	12	0.00875	297.1
[7]	0.8~2.7	26.6	0.00211	900.5
[13]	1.35~3.5	21.6	0.00456	471.5
[14]	0.86~0.96	20	0.00023	434.8
This paper	0.68~2.13	6	0.00044	3295.5

Tab. 1. Comparison between the proposed MA and absorbers in reference.

4. Conclusion

In conclusion, we have designed and fabricated a tunable MA which performed broadband absorption at low-frequency controlled by the bias voltage. By establishing the TL model, we obtained the function of the resonance frequency, real part of input impedance and loaded. To demonstrate the tunability and strong absorption, we analyzed ST coefficients to the unit cell pattern. The calculated results suggest that the capacitance modulates the imaginary part of the input impendence, producing the tunability, while the resistor mainly adjusts real part, producing the strong absorption. For further optimization of ST coefficients, we realized that the value of x and y effectively expand the tunable bandwidth. Finally, we measured the reflectivity curves of MA for different voltage. Measurement results show that the structure can be tuned to provide a continuously variable reflectivity level of less than –10 dB from 0.68 to 2.13 GHz, and the total thickness 6 mm is only $\lambda/31$ of the center frequency. Measurements are in good agreement with results obtained from simulations. The proposed MA shows great promise for a variety of application such as detectors and solar cells in the future.

Acknowledgments

This work was supported by the Postdoctoral Innovative Talents Support Program of China (Grant No. BX20180375), the National Natural Science Foundation of China (Grant Nos. 61801508, 61701523, 61671464, and 61471389), and the Natural Science Basic Research Program of Shaanxi Province, China (Grant Nos. 2019JQ-103 and 2018JM6040).

References

[1] LANDY, N. I., SAJUYIGBE, S., MOCK, J. J., et al. Perfect metamaterial absorber. *Physical Review Letters*, 2006, vol. 100, no. 20, p. 1–4. DOI: 10.1103/PhysRevLett.100.207402

[2] WATTS, C. M., LIU, X. L., PADILLA, W. J. Metamaterial electromagnetic wave absorbers. *Advanced Materials*, 2012, vol. 24, no. 23, p. 98–120. DOI: 10.1002/adma.201200674

[3] YUAN, W. CHENG, Y. Low-frequency and broadband metamaterial absorber based on lumped elements: Design, characterization and experiment. *Applied Physics A*, 2014, vol. 117, no. 4, p. 1915–1921. DOI: 10.1007/s00339-014-8637-3

[4] HAN, Y., CHE, W. Q. Low-profile broadband absorbers based on capacitive surfaces. *IEEE Antennas and Wireless Propagation Letters,* 2017, vol. 16, p. 74–78. DOI: 10.1109/LAWP.2016.2556753

[5] LI, X. S. J., CAO, Y., GAO, J., et al. Analysis and design of three-layer perfect metamaterial-inspired absorber based on double split-serration-rings structure. *IEEE Transactions on Antennas and Propagation*, 2015, vol. 63, no. 11, p. 5155–5160. DOI: 10.1109/TAP.2015.2475634

[6] LI, S. J., WU, P. X., XU, H. X., et al. Ultra-wideband and polarization-insensitive perfect absorber using multilayer metamaterials, lumped resistors and strong coupling effects. *Nanoscale Research Letters*, 2018, vol. 13, p. 1–13. DOI: 10.1186/s11671-018-2810-0

[7] ZUO, W. Q., YANG, Y., HE, X. X., et al. An ultrawideband miniaturized metamaterial absorber in the ultrahigh-frequency range. *IEEE Antennas and Wireless Propagation Letters*, 2017, vol. 16, p. 928–931. DOI: 10.1109/LAWP.2016.2614703

[8] LEE, J., LIM, S. Bandwidth-enhanced and polarisation-insensitive metamaterial absorber using double resonance. *Electronics Letters*, 2011, vol. 47, no. 1, p. 8–9. DOI: 10.1049/el.2010.2770

[9] GU, S., SU, B., ZHAO, X. P. Planar isotropic broadband metamaterial absorber. *Journal of Applied Physics,* 2013, vol. 114, no. 16, p. 1–6. DOI: 10.1063/1.4826911

[10] SHANG, S., YANG, S. Z., TAO, L., et al. Ultrathin triple-band polarization-insensitive wide-angle compact metamaterial absorber. *AIP Advances,* 2016, vol. 6, no. 7, p. 1–8. DOI: 10.1063/1.4958660

[11] ZHONG, H. T., YANG, X. X., TAN, C., et al. Triple-band polarization-insensitive and wide-angle metamaterial array for electromagnetic energy harvesting. *Applied Physics Letters*, 2016, vol. 109, no. 25, p. 1–4. DOI: 10.1063/1.4973282

[12] ZHU, J. F., MA, Z. F., SUN, W. J., et al. Ultra-broadband terahertz metamaterial absorber. *Applied Physics Letters*, 2014, vol. 105, no. 2, p. 1–4. DOI: 10.1063/1.4890521

[13] BANADAKI, M. D., HEIDARI, A. A., NAKHKASH, M. A metamaterial absorber with a new compact unit cell. *IEEE Antennas and Wireless Propagation Letters,* 2018, vol. 17, no. 2, p. 205–208. DOI: 10.1109/LAWP.2017.2780231

[14] ZUO, W. Q., YANG. Y., HE, X. X., et al. A miniaturized metamaterial absorber for ultrahigh-frequency RFID system. *IEEE Antennas and Wireless Propagation Letters*, 2017, vol. 16, p. 329–332. DOI: 10.1109/LAWP.2016.2574885

[15] XU, W. H., HE, Y., KONG, P., et al. An ultra-thin broadband active frequency selective surface absorber for ultrahigh-frequency applications. *Journal of Applied Physics,* 2015, vol. 118, no. 18, p. 1–8. DOI: 10.1063/1.4934683

[16] AZAD, A. K., TAYLOR, A. J., SMIRNOVA, E., et al. Characterization and analysis of terahertz metamaterials based on rectangular split-ring resonators. *Applied Physics Letters,* 2008, vol. 92, no. 1, p. 1–3. DOI: 10.1063/1.2829791

[17] FU, L., SCHWEIZER, H., GUO, H., et al. Synthesis of transmission line models for metamaterial slabs at optical frequencies. *Physical Review B,* 2008, vol. 78, no. 11, p. 1–9. DOI: 10.1103/PhysRevB.78.115110

About the Authors …

GuoWen ZHANG was born in ChongQing Municipality, in 1995. He received the B. S. degree from the Information and Navigation College, Air Force Engineering University in 2017. He is now a graduate student. His research interest is in electromagnetic metamaterial. He has been working with the EMC Lab, since 2017. His research activity has been focused in the broadband and fractal artificial magnetic conductor, coding metamaterial and its application for RCS reduction of antennas.

Jun GAO received the B.Sc and M.A.Sc degrees from the Air Force Missile Institute in 1984 and 1987, respectively. He joined the Air Force Missile Institute in 1987 as an assistant teacher. He became an associate professor in 2000. He is currently a professor of the Information and Navigation College, Air Force Engineering University of CPLA.

He has authored and coauthored more than 100 technical journal articles and conference papers, and holds one China soft patent. His research interests include smart antennas, electromagnetic metamaterial and their antenna applications.

Xiangyu CAO received the B. Sc and M.A. Sc degrees from the Air Force Missile Institute in 1986 and 1989, respectively. She joined the Air Force Missile Institute in 1989 as an assistant teacher. She became an associate professor in 1996. She received Ph.D. degree in the Missile Institute of Air Force Engineering University in 1999. From 1999 to 2002, she was engaged in postdoctoral research in Xidian University, China. She was a Senior Research Associate in the Dept. of Electronic Engineering, City University of Hong Kong from June 2002 to Dec 2003. She is currently a professor of the Information and Navigation College of the Air Force Engineering University of CPLA. She is the IEEE senior member from 2008. She has authored and coauthored more than 200 technical journal articles and conference papers, and holds one China soft patent. She is the coauthor of two books entitled Electromagnetic Field and Electromagnetic Wave, and Microwave Technology and Antenna published in 2007 and 2008, respectively. Her research interests include smart antennas, electromagnetic metamaterial and their antenna applications, and electromagnetic compatibility. She is a reviewer of Applied Physics Letter, Journal of Applied Physics, IEEE Transactions on Antennas & Propagation, and IEEE Antennas Wireless Propagation Letter.

HuanHuan YANG has received the M. Eng. degree in Electronic Science and Technology from the Air Force Engineering University, Xi'an China, in 2012. His research activity has been focused in polarized reconfigurable antenna He has authored and coauthored more than 30 scientific papers in major journals and international conferences. His research activity has been focused in the broadband perfect metamaterial absorber and its application for RCS reduction of antennas. He is a reviewer of Applied Physics Letter, Journal of Applied Physics, IEEE Transactions on Microwave Theory & Techniques, IEEE Transactions on Antennas & Propagation, IEEE Antennas Wireless Propagation Letter, Electronic Letters and Microelectronics Journal.

Liaori JIDI was born in SiChuan province in 1994. He received the B. S. degree from the Information and Navigation College, Air Force Engineering University in 2017. He is now a graduate student. His research interest is in electromagnetic metamaterial. He has been working with the EMC Lab. His research activity has been focused in the broadband perfect metamaterial absorber and its application for RCS reduction of antennas.